

MODELLING NaCl CONCENTRATION PROFILES  
ACROSS A CATION EXCHANGE MEMBRANE IN THE  
TRANSIENT REGIME

Victor Verbist

Delft, 21st June 2019

Bachelor End Project,  
Applied Physics & Applied Mathematics,  
TU Delft

Supervisors:  
Prof.dr.ir. C. Vuik  
Prof.dr. B. Dam

Daily supervisor:  
M.A. Blommaert

## Abstract

A model is developed to simulate NaCl concentrations across a cation exchange membrane in the transient regime. The convectionless Nernst-Planck equation is combined with the continuity equation to obtain a partial differential equation in time and space. The boundary conditions at the edges of the cell for this equation are a constant bulk concentration. Furthermore, in presence of an applied potential, the potential gradient is assumed to be linear with different values for the gradient inside and outside the membrane. This different value inside the membrane is due to Donnan potentials that arise at the membrane/electrolyte interfaces. On top of this, because of the Donnan exclusion, the concentrations are not continuous on the interface. To account for this, the cell is split into three regions: the membrane and two electrolyte regions on either side of the membrane. The boundary conditions to tie these regions together, is that the flux should be continuous across the interface. The problem has the form of an initial value problem. The partial differential equation is discretized using a finite difference method and is integrated using the forward Euler method.

The results show an accumulation of ions at the membrane interface closest to the positive electrode, while ions are depleted at the other interface. This accumulation of ions is too big however, with the  $Na^+$  concentration at one point reaching 12M after only 0.10 seconds, while the concentration was 1M at the start. This is clearly not what one would expect to happen physically. There were, however, no errors found in the numerical method as it was possible to correctly deduce and predict concentration changes, based on the concentrations and flux in a certain time step. Therefore it appears that there is an error in the assumptions that were made when developing the model. It is believed that this error lies in the assumption that the potential gradients only has two different values. This assumption ignores the diffusion boundary layers on the outside of the membrane. In this diffusion boundary layer, the potential gradient has another, different value. Therefore, to obtain more accurate results, the cell should actually be split into five different regions: the membrane, two diffusion boundary layers and two electrolyte solutions.

# Contents

<b>1</b>	<b>Introduction</b>	<b>1</b>
<b>2</b>	<b>Theory</b>	<b>2</b>
2.1	Electrochemical cell . . . . .	2
2.2	Ion Transport . . . . .	3
2.2.1	Diffusion . . . . .	3
2.2.2	Migration . . . . .	3
2.2.3	Convection . . . . .	4
2.2.4	Nernst-Planck Equation . . . . .	4
2.2.5	Electrical Current . . . . .	4
2.2.6	Electroneutrality . . . . .	5
2.3	Ion Exchange Membranes . . . . .	5
2.4	Donnan Equilibrium and Donnan Potential . . . . .	6
2.4.1	Potential profile across an ion exchange membrane . . . . .	7
2.5	Continuity Equation . . . . .	8
2.6	Finite Difference Method . . . . .	9
2.6.1	Numerical Derivatives . . . . .	9
2.6.2	Numerical integration of initial value problems . . . . .	10
2.6.3	Example: heat equation . . . . .	11
2.7	Newton-Raphson approximation method . . . . .	12
2.8	Literature Study . . . . .	13
<b>3</b>	<b>Model Development and Numerical Method</b>	<b>14</b>
3.1	Problem Description . . . . .	14
3.2	Physical Model . . . . .	15
3.2.1	Initial Condition: no electric field . . . . .	15
3.2.2	Partial Differential Equation for the concentration . . . . .	15
3.2.3	Boundary Conditions . . . . .	17
3.3	Numerical Model . . . . .	17
3.3.1	Discretization of the system . . . . .	17
3.3.2	Region I . . . . .	18
3.3.3	Region III . . . . .	19
3.3.4	Region II . . . . .	20
3.3.5	Electrolyte/membrane interface . . . . .	21
<b>4</b>	<b>Results</b>	<b>22</b>
4.1	Parameters . . . . .	22
4.2	No Applied Potential . . . . .	23
4.3	Applied Potential . . . . .	23
<b>5</b>	<b>Discussion</b>	<b>27</b>
5.1	No applied potential . . . . .	27
5.2	Applied Potential . . . . .	27
<b>6</b>	<b>Conclusion</b>	<b>30</b>
	<b>References</b>	<b>31</b>

# 1 Introduction

In a lot of chemical applications, ion exchange membranes are used. These are a type of membrane that facilitate a certain type of ions to pass through it: either positive ions or negative ions. Ion exchange membranes have a lot of applications, for example in (reverse) electrodialysis, seawater desalination and batteries [1]. Ideally, such a membrane allows *only* positive or negative ions to pass through and not the other type. In practice, however, also some ions of the 'wrong' type are transported through the membrane, a process called co-ion crossover. In most applications, this co-ion crossover is not beneficial. Therefore it is vital to understand how concentrations change across a membrane, specifically in the presence of an applied electrical field. This could make for a better understanding as to why co-ion crossover happens and help find ways to prevent it from happening.

This project aims to simulate the concentration profiles across an ion exchange membrane in the transient regime. That is, a model is written which calculates the concentrations profiles at different time steps. The simulated cell consists of a cation exchange membrane in a NaCl solution. The starting situation is a situation where there is no applied voltage. Then a voltage is applied and it is simulated how the concentrations change with every time step. Key concepts in the model are the Nernst-Planck equation, Donnan exclusion, the continuity equation and the finite element method.

This report is structured as follows. First, the theory of the physics and numerical methods involved is explained. Then there is a section that presents the physics and equations that describe the problem, as well as how to turn that into a numerical model. After that, the results are presented, followed by a section where these results are discussed. Finally, in the last section, conclusions are drawn about the results of the model.

This project is a bachelor end project for the double bachelor Applied Physics and Applied Mathematics at Delft University of Technology. The supervisors are prof.dr.ir C. Vuik (Numerical Analysis, Applied Mathematics, EEMCS, TU Delft) and prof.dr. B. Dam (MECS, Chemical Engineering, Applied Sciences, TU Delft). The daily supervisor of the project is M.A. Blommaert.

## 2 Theory

### 2.1 Electrochemical cell

Electrochemistry is the study of chemical change in combination with electricity. More generally, it describes the (redox) reactions in a so called electrochemical cell. Such a cell consists of the following: the electrolyte (an ionic solution), two or more electrodes and an electrical circuit, which connects the two electrodes, see figure 1. The electrode/electrolyte interface is very important in such an

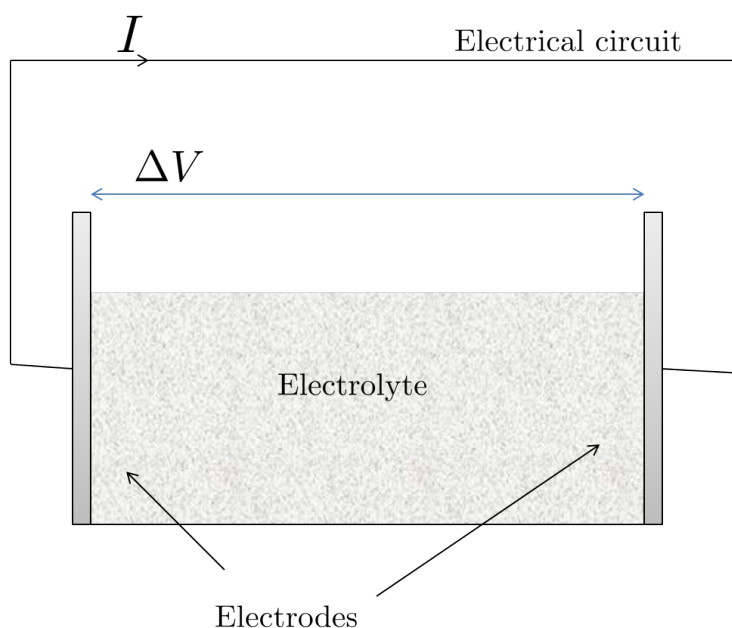


Figure 1: An electrochemical cell consists of three things: an electrolyte, two electrodes and an electrical circuit, which connects the two electrodes. There is a potential difference  $\Delta V$  over the cell and a current  $I$  through the circuit.

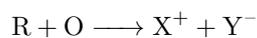
electrochemical cell. This is because the electrolyte is an *ionic* conductor and the electrode and circuit are *electronic* conductors. The interface of these two is then a place where ions and electrons come together and thus a reaction between the two can occur. These reactions, involving a molecule or ion and an electron, can be categorized into two different groups: reduction reactions and oxidation reactions. Reduction is when a molecule or ion reacts with an electron, i.e. it gains an electron.



Oxidation is when a molecule or ion loses an electron.



These are called half reactions. Adding them both yields the overall reaction:



where electrons are transported from the oxidizing agent to the reducing agent.

This process is exploited in an electrochemical cell. When two different half reactions occur at the two different electrodes, then electrons travel through the electrical circuit that connects the two electrodes. In this way, an electrical current is generated, opposite to the flow of electrons. From this, it can be seen that what happens at one electrode, influences what happens at another electrode. Thus to be able to understand what is going on in an electrochemical cell, it is not sufficient to look at the single interfaces. Instead, the whole cell should be examined [2].

There are two types of electrochemical cells: galvanic cells and electrolytic cells. In galvanic cells, the half reactions at the electrode/solution interfaces occur spontaneously. This means that a current is generated, as soon as the electrodes are connected by a conductor. The chemical energy of the cell is converted to electrical energy. An electrolytic cell is the exact opposite. The reactions are not spontaneous, instead an external voltage source is connected to the electrodes. If the applied voltage is big enough, the reactions will occur. Thus in an electrolytic cell, electrical energy is converted to chemical energy. It is possible to think of an electrolytic cell as a cell that is being charged, while a galvanic cell is being discharged. This mechanism is comparable to charging and using a battery.

## 2.2 Ion Transport

Generally there are three transport methods for ions in a solution [2]. These are diffusion, migration and convection, caused by a concentration gradient, electric potential gradient and pressure gradient, respectively. Ion transport is described by ion flux: the amount of ions that flow through a certain area in a certain time period. As such, ion flux has dimensions  $\text{mol m}^{-2} \text{s}^{-1}$ .

### 2.2.1 Diffusion

Diffusion is caused by a difference in chemical potential (i.e. a concentration difference over a certain distance, called the concentration gradient) [3]. The flux  $J$  of an ion species, as a result of this diffusion, is described by Fick's Law:

$$J = -D \frac{dc}{dx} \quad (1)$$

Here  $J$  has units  $\text{mol m}^{-2} \text{s}^{-1}$ ,  $D$  is the diffusion coefficient ( $\text{m}^2 \text{s}^{-1}$ ) and  $c$  denotes the concentration (M). Note that an equivalent equation holds in two or three dimensions, then the derivative must be replaced by the more general gradient operator  $\nabla$ :

$$\mathbf{J} = -D \nabla c \quad (2)$$

### 2.2.2 Migration

Because ions are charged particles, they are susceptible to an electric field gradient. Positive ions will be transported away from positive sources towards negative ones and negative ions vice versa. This mass transfer caused by an

electric field gradient, is called migration. The migrational flux is proportional to the concentration and the electric field gradient:

$$J \propto c \frac{d\phi}{dx} \quad (3)$$

As it turns out, it is possible to express the proportionality constant in the diffusion coefficient  $D$  from Fick's law [2]:

$$J = -\frac{zF}{RT} Dc \frac{d\phi}{dx} \quad (4)$$

In this equation,  $z$  is the sign of the ion species (-),  $F \approx 96485 \text{ C mol}^{-1}$  is the Faraday constant,  $R \approx 8.314 \text{ J mol}^{-1} \text{ K}^{-1}$  is the gas constant and  $T$  is the temperature in Kelvin [4]. Again, this equation can be generalised to multiple dimensions:

$$\mathbf{J} = -\frac{zF}{RT} Dc \nabla \phi \quad (5)$$

### 2.2.3 Convection

The third method of mass transportation is convection. The driving force for this is a pressure (or density) gradient or an external driving force, like a stirrer. As a result of a pressure difference, the solution will flow, namely from a high pressure area to a low pressure area. The ions, that are solved in this solution, will then naturally follow the same flow. The mass transfer  $J$  is then simply the concentration  $c$  times the velocity  $v$  ( $\text{ms}^{-1}$ ):

$$J = cv \quad (6)$$

This result can be extended to multiple dimension, with  $J$  and  $v$  being vectors.

### 2.2.4 Nernst-Planck Equation

Now the total mass transportation is the sum of the contributions from diffusion, migration and convection:

$$J = -D \frac{dc}{dx} - \frac{zF}{RT} Dc \frac{d\phi}{dx} + cv \quad (7)$$

This result is known as the Nernst-Planck equation and is one of the most important equations in studying ion transport. In a lot of cases, the convection term is neglected because it is too small relative to the diffusion and migration terms. Again, a 2D or 3D equivalent of equation 7 can be obtained by substituting the spatial derivatives  $\frac{d}{dx}$  for the gradient  $\nabla$ .

$$\mathbf{J} = -D \nabla c - \frac{zF}{RT} Dc \nabla \phi + \mathbf{c}v \quad (8)$$

### 2.2.5 Electrical Current

It is possible to relate the flux  $J$  to an electrical current  $I$ . Current is namely defined as the rate at which electric charge flows through a surface area, with units Ampere (C/s). Using the fact that the charge in Coulomb of a mole

of electrons is equal to Faradays constant  $F \approx 96458 \text{ C mol}^{-1}$ , the following expression for the current through a surface with area  $A$  is obtained:

$$I = zJFA \quad (9)$$

If there are multiple ions in a solution, the total current is the sum of the contributions from the different species  $i$ :

$$I = \sum_i I_i = \sum_i z_i J_i F A \quad (10)$$

### 2.2.6 Electroneutrality

Another important phenomenon in the transport of ions is electroneutrality. While it is possible for ions to have a charge, a solution must always (locally) be electrically neutral in the bulk of a solution. This means that for every positive ion in the bulk, there must be a negative ion nearby. This can be summarised as follows:

$$\sum_i z_i c_i(x) = 0 \quad (11)$$

## 2.3 Ion Exchange Membranes

In a lot of practical applications, for example (reverse) electrodialysis, ion exchange membranes (IEMs) are used [5]. These are a type of permselective membranes which are highly permeable to ions of a certain charge, while hardly permeable to ions of the opposite charge [1]. Thus there are two different types: cation exchange membranes (CEM) and anion exchange membranes (AEM). A CEM is mostly permeable to cations (positively charged ions) while an AEM is mostly permeable to anions (negatively charged ions). These are called the counter-ions, for they have a charge opposite in sign to the membrane. Likewise, the ions that an IEM is hardly permeable to are called co-ions.

The way this works, is that IEMs have fixed, ion groups of a certain charge, see figure 2 [6]. In a CEM these groups have negative charge, such that there are mobile positive ions in the membrane. In this way cations move rather easily across the membrane, while anions are impeded. For AEMs this is reversed: the fixed charge groups are positive which facilitates anion transport.



Figure 2: Ion exchange membranes. Due to the negatively charged fixed ion groups of a CEM, cations permeate easily while anions are impeded. The reverse is true for an AEM. [6]

The concentration of these fixed groups is an important characteristic of IEMs and is usually denoted by the letter  $X$  (M). Because of electroneutrality, the

following condition holds inside the membrane:

$$\sum_i z_i c_i \pm X = 0 \quad (12)$$

where there should be a plus sign for an AEM (positive fixed charge groups) and a minus sign for a CEM (negative fixed charge groups).

## 2.4 Donnan Equilibrium and Donnan Potential

As described in the previous section, a CEM is relatively permeable for cations, while it excludes anions. This phenomenon is called Donnan Exclusion and when the solution outside the membrane is in electrochemical equilibrium with the inner solution, there is a Donnan equilibrium [1]. This leads to a condition, derived from the theory of Teorell, Meyer and Sievers, for the concentrations at the membrane interface.

Before this condition is presented, it is useful to introduce some notation. A horizontal bar over a quantity indicates the value of that quantity *inside* the membrane. Furthermore the symbol  $\nu$  is used. This signifies that an electrolyte dissociates into  $\nu_C$  mole of cation and  $\nu_A$  of anion.

Now, the condition that follows from the electrochemical equilibrium across the membrane interface, reads as follows [1]:

$$\bar{c}_C^{\nu_C} \cdot \bar{c}_A^{\nu_A} = c_C^{\nu_C} \cdot c_A^{\nu_A} \quad (13)$$

For a NaCl-solution, this yields:

$$\bar{c}_{Na} \cdot \bar{c}_{Cl} = c_{Na} \cdot c_{Cl} \quad (14)$$

By electroneutrality  $\bar{c}_{Na} = \bar{c}_{Cl} + X$ , for a CEM. When this is substituted in equation 14, the following expression for the concentrations inside the membrane can be obtained:

$$\bar{c}_{Na} = \frac{1}{2} \left( \sqrt{X^2 + 4c_{Na}c_{Cl}} + X \right) \quad (15)$$

$$\bar{c}_{Cl} = \frac{1}{2} \left( \sqrt{X^2 + 4c_{Na}c_{Cl}} - X \right) \quad (16)$$

In this way, the Na- and Cl-concentrations can be easily computed, given the concentrations near the membrane and the fixed charge concentration of the membrane. In the case of a NaCl-solution, the Na- and Cl- concentrations must be equal outside of the membrane, because of electroneutrality. But inside the membrane, these concentrations differ. This phenomenon is called concentration polarization.

As a consequence of this concentration polarization, an electric potential is generated across the membrane interface. This is called the Donnan potential and can be computed as follows [1]:

$$E_{Don} = \frac{RT}{F} \ln \frac{\bar{c}_i}{c_i} \quad (17)$$

where the subscript  $i$  denotes that it is the concentration of the *counter-ion* (so in the previous example, this would be Na).  $R$  is the gas constant,  $T$  the temperature in Kelvin and  $F$  is Faraday's constant.

### 2.4.1 Potential profile across an ion exchange membrane

It is interesting to see what the potential across the ion exchange membrane looks like, when this Donnan potential is taken into account. In the electrolyte, so outside of the membrane, a linear potential profile is expected (far away enough from the electrodes). This linear potential comes from the applied potential across the electrodes. But due to the Donnan potential, there is a 'jump' in potential at the solution/membrane-interfaces, as shown in figure 3.

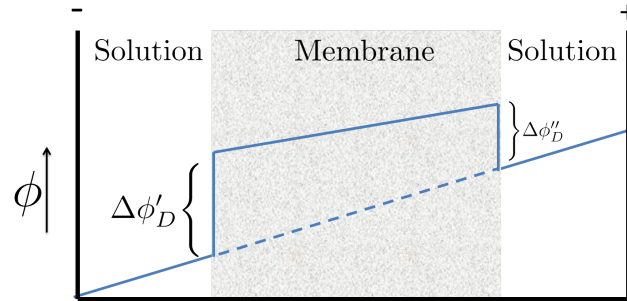


Figure 3: The potential  $\phi$  across an ion exchange membrane. There is a linear potential due to the potential difference between the electrodes and on the membrane interfaces, there is a potential jump due to the Donnan potential.

The results of this section are summarized in figure 4.

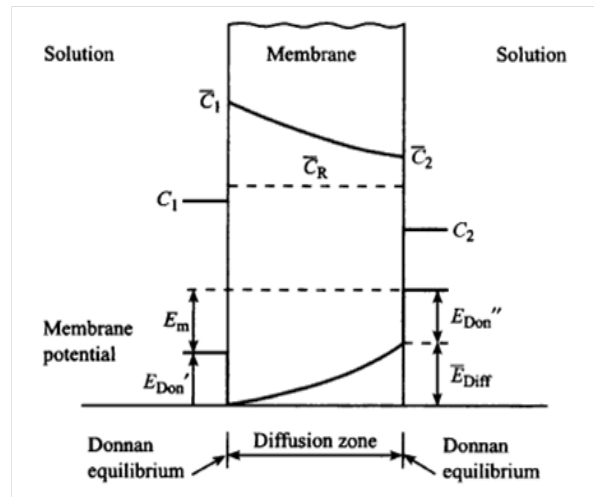


Figure 4: Schematic figure of an ion exchange membrane. The concentrations denote the concentration of the counter-ion.  $\bar{c}_R$  is the magnitude of the fixed charged concentration. The electric potential is also shown. [1]

## 2.5 Continuity Equation

It is possible to derive a partial differential equation (PDE) of the concentration in a solution in time and space using the flux. In this section, it is done for one dimension, but it is also possible to generalise to multiple dimensions. To obtain this PDE, consider a volume element in the solution, at location  $x$ , of width  $\Delta x$  and cross-section area  $A$ , perpendicular to the  $x$ -axis, see figure 5.

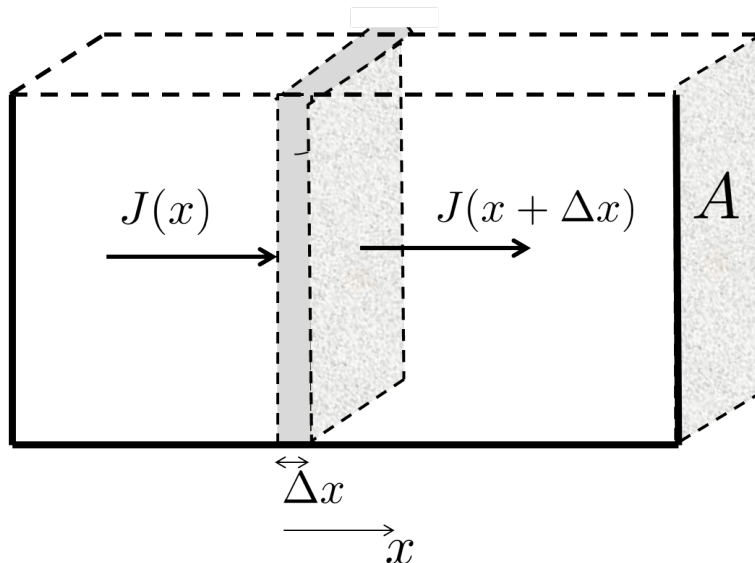


Figure 5: Flux  $J$  into and out of a volume element with width  $\Delta x$  and cross section area  $A$ .

Clearly, mass is a conserved quantity, which is to say that there is no mass created or destroyed in the solution. Then, it should hold that the change of mass in this volume element, is equal to the mass flux into the volume, minus the mass flux out of the volume, multiplied with the area  $A$  over which the flux enters or exits:

$$\frac{\partial m}{\partial t} = J(x) \cdot A - J(x + \Delta x) \cdot A \quad (18)$$

Here  $J(x)$  denotes the mass flux at position  $x$ . The amount of mass  $m$  is equal to the concentration times the volume:

$$m = c \cdot V = c \cdot A \Delta x \quad (19)$$

Substituting this in equation 18 yields:

$$\frac{\partial c \cdot A \Delta x}{\partial t} = J(x) \cdot A - J(x + \Delta x) \cdot A \quad (20)$$

Note that both  $A$  and  $\Delta x$  do not change in time, such that:

$$A \Delta x \frac{\partial c}{\partial t} = J(x) \cdot A - J(x + \Delta x) \cdot A \quad (21)$$

Which can be rewritten as:

$$\frac{\partial c}{\partial t} = - \frac{J(x + \Delta x) - J(x)}{\Delta x} \quad (22)$$

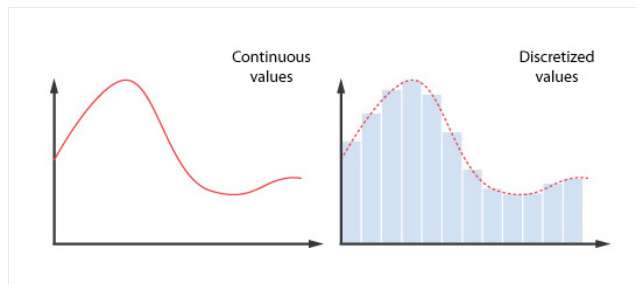


Figure 6: Discretization of a function [7].

Taking the limit of  $\Delta x \rightarrow 0$ , the fraction on the right hand side of equation 22 is exactly the definition of the partial derivative of  $J$  in the  $x$ -direction:

$$\frac{\partial c}{\partial t} = -\frac{\partial J}{\partial x} \quad (23)$$

This result is known as the continuity equation and plays an important role in modelling physical transport phenomena. Just as in previous sections, this result can be generalised to hold in multiple dimensions:

$$\frac{\partial \mathbf{c}}{\partial t} = -\nabla \mathbf{J} \quad (24)$$

In many cases however, it is very difficult to obtain an analytical solution to a partial differential equation such as (23) or (24). Therefore numerical methods are often used to solve these types of equations. One such method is the finite difference method.

## 2.6 Finite Difference Method

In almost all cases, it is too difficult to calculate concentration profiles analytically. Therefore numerical methods have to be used. One of the most used techniques is the finite difference method, also called the finite element method. In this method, the system is discretized using a grid. So instead of a continuous (analytical) function for the concentration on the domain, the concentrations are determined in a finite number of points. This is illustrated in figure 6. This technique is especially useful when working with (partial) differential equations. That is because derivatives in a certain point can be easily approximated using other points around that original point.

### 2.6.1 Numerical Derivatives

Using only the values of a function in the grid points, it is possible to determine the derivative of that function, in these grid points [8]. Consider for example a function  $f(x)$  on some interval  $[0, L]$  that is discretized in a grid of  $n + 1$  points  $(x_0, \dots, x_n)$ . Then  $x_0 = 0$  and  $x_n = L$  with a constant spacing of  $\Delta x = \frac{L}{n}$  between two consecutive points. Now there are multiple ways to approximate the derivative of  $f$  in a point  $x_i$ :

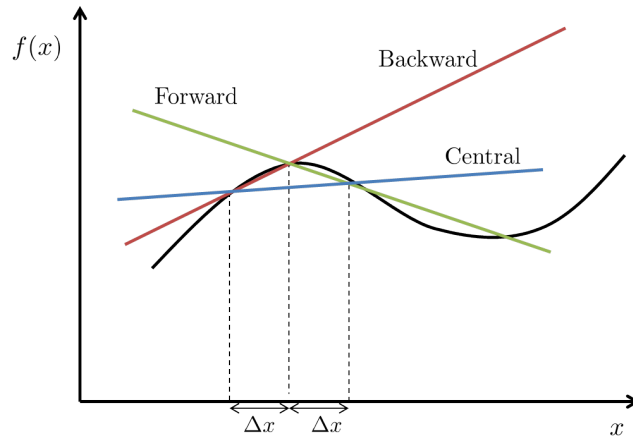


Figure 7: Illustration of a forward, backward and central difference to approximate a derivative.

$$\begin{aligned} \text{forward difference:} & \quad \frac{f(x_{i+1}) - f(x_i)}{\Delta x} \\ \text{backward difference:} & \quad \frac{f(x_i) - f(x_{i-1})}{\Delta x} \\ \text{central difference:} & \quad \frac{f(x_{i+1}) - f(x_{i-1})}{2\Delta x} \end{aligned}$$

The different approximations are pictured in figure 7. It is also possible to approximate second order derivatives. While there exist many ways to do this, it is common practice to use a central difference method:

$$\frac{f(x_{i+1}) - 2f(x_i) + f(x_{i-1}))}{\Delta x^2}$$

Actually, it is possible to approximate any order derivative and there are multiple ways to do so. For now, however, only first and second order derivatives are relevant.

The most important property of these numerical derivatives, is that they can all be computed making use of the function values. That means there is no difficult algebra or calculus involved. In fact, the derivatives are often linear combinations of the function values, a characteristic that will be convenient later.

### 2.6.2 Numerical integration of initial value problems

In the previous section, it was shown how to approximate derivatives using finite difference methods. It is however also possible to 'integrate' in this way and this technique is used particularly in solving (partial) differential equations. Consider for example a forward difference time derivative:

$$f'(t_j) \approx \frac{f(t_{j+1}) - f(t_j)}{\Delta t}$$

Rearranging the terms, then gives:

$$f(t_{j+1}) \approx f(t_j) + \Delta t f'(t_j)$$

The interesting part here, is that if there is information (the value of the function and that of the derivative) about  $f$  at a certain time  $t_j$ , it is possible to compute

the value of  $f$  at a *different* time  $t_{j+1}$ . The way in which that is done here above, using a forward difference, is called the Euler method.

Using a backwards difference, one obtains the backward Euler method:

$$f'(t_{j+1}) \approx \frac{f(t_{j+1}) - f(t_j)}{\Delta t}$$

$$f(t_{j+1}) + \Delta t f'(t_{j+1}) \approx f(t_j)$$

Note that this however gives an implicit expression for  $f(t_{j+1})$ , because one also needs the derivative of  $f$  in  $t_{j+1}$ . This would suggest that the Euler method is a 'better' method, because this gives a simpler, explicit expression for  $f(t_{j+1})$ . The Backwards Euler method, however, offers a different benefit. This benefit is that the backwards Euler method is stable for far more values of  $\Delta t$  than the forward Euler method. While stability is an important property of certain numerical methods, it will not be investigated further in this section.

Next, the concepts above are illustrated with an example.

### 2.6.3 Example: heat equation

To illustrate the benefits of the finite difference method, the temperature  $u$  as a function of position  $x$  and time  $t$  in a uniform 1D rod is studied. The partial differential equation that describes the temperature  $u(x, t)$  in this rod is called the heat equation:

$$\frac{\partial u}{\partial t} = \frac{\partial^2 u}{\partial x^2} \quad (25)$$

The rod has a length  $L$  and the temperatures at the boundaries are constant in time:

$$u(x = 0, t) = A$$

$$u(x = L, t) = B$$

Furthermore, the initial temperature of the rod is given by some function  $g(x)$ :

$$u(x, t = 0) = g(x)$$

The goal is to describe the temperature at different positions in the rod, at different times. If the temperature is known at a certain time  $t_0$ , then the temperature a time step  $\Delta t$  later can be calculated using the Euler method:

$$u(x, t = t_0 + \Delta t) \approx u(x, t_0) + \Delta t \frac{\partial u}{\partial t}(x, t_0) = u(x, t_0) + \Delta t \frac{\partial^2 u}{\partial x^2}(x, t_0) \quad (26)$$

where in the last step the heat equation (25) is used. To find  $\frac{\partial^2 u}{\partial x^2}(x, t_0)$ , a numerical derivative can be used, given that the temperature at time  $t_0$  is known. In order to do this, the length is discretized in  $n + 1$  parts of width  $\Delta x = \frac{L}{n+1}$ . The grid points are then  $x_i = i\Delta x$  for  $i = 0, \dots, n + 1$ , such that  $x_0 = 0$  and  $x_{n+1} = L$ . For example a central difference can be used:

$$\frac{\partial^2 u}{\partial x^2}(x_i, t_0) \approx \frac{u_{i+1} - 2u_i + u_{i-1}}{\Delta x^2}$$

Here  $u_i$  corresponds to  $u(x_i, t_0)$  for cleaner notation. Furthermore, at the boundaries the temperatures are constant:  $u_0 = A$  and  $u_{n+1} = B$ . An important



roots with every iteration. An initial guess  $x_0$  is made for the root and the next guess  $x_1$  is determined as follows:

$$x_1 = x_0 - \frac{f(x_0)}{f'(x_0)} \quad (32)$$

The next, improved, guess is then computed similarly. So in general:

$$x_{k+1} = x_k - \frac{f(x_k)}{f'(x_k)} \quad (33)$$

This process is then stopped whenever  $f(x_k) = 0$  for some  $k$  or when some stopping criterion is met. One example of such a stopping criterion is when the difference between two successive guesses is relatively small, such that approximating it any further won't result in a significantly different value.

This method converges quadratically to the right answer, if  $f(x)$  satisfies the following conditions [9]:

1.  $f'(x) \neq 0$
2.  $f''(x)$  is continuous
3. The initial guess  $x_0$  is close enough to the true value of the root

This method can also be extended to solve a system of equations  $\mathbf{F} = \mathbf{0}$ . The iteration then looks as follows:

$$\mathbf{x}_{k+1} = \mathbf{x}_k - J_F^{-1}(\mathbf{x}_k)F(\mathbf{x}_k) \quad (34)$$

Where  $J_F$  is the Jacobian of  $\mathbf{F}$ :

$$J_F(\mathbf{x}) = \begin{bmatrix} \frac{\partial F_1}{\partial x_1} & \dots & \frac{\partial F_1}{\partial x_n} \\ \vdots & \ddots & \vdots \\ \frac{\partial F_n}{\partial x_1} & \dots & \frac{\partial F_n}{\partial x_n} \end{bmatrix} \quad (35)$$

## 2.8 Literature Study

There are many studies available that aim to model the concentration profiles inside and around an ion exchange membrane. For example, [10] describes a model of a CEM in a NaCl-concentration, under the influence of an electric field gradient, which is in agreement with experimental results. Though, in the article it is assumed that the membrane is ideally permselective, i.e. there are no co-ions inside the membrane. This assumption, however, is only valid for low concentrations. It would be interesting to know what happens when a CEM is placed in a higher concentration where co-ion crossover is present to a greater extent. Furthermore, [11] and [12] have developed a model for concentrations in a (reverse) electrodialysis process, where there is made heavy use of IEMs. Especially [12] is interesting, as the only input parameters are the geometrical features of the system, the fixed charge group concentrations of the membranes and the diffusion coefficient of the ions. In this study though, the calculations have been done for a steady state problem and the aim of the present work is to describe a transient problem. Nevertheless, [12] provides useful insights to do this and this work will follow a similar approach.

### 3 Model Development and Numerical Method

This section aims to describe how the model is developed. First a problem description is given. Then the equations that describe the problem are developed, as well as the relevant boundary conditions. This is the 'physical' model. After this, it is shown how to translate this into a 'mathematical/numerical' model, which can be interpreted by an algebraic equation solver, such as Matlab or Python. Key concepts in this numerical model are the finite difference method and forward Euler integration.

#### 3.1 Problem Description

The goal of the model is to describe concentration profiles inside an electrochemical cell with an ion exchange membrane (IEM). The researched cell consists of a NaCl-solution as electrolyte and a cation exchange layer (CEL) for the IEM. Furthermore, an electric field is applied across the cell, see figure 8.

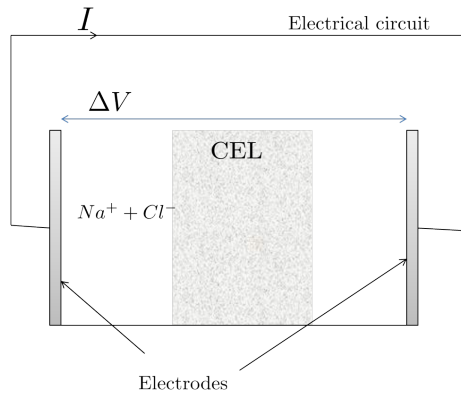


Figure 8: An electrochemical cell with a NaCl-solution as electrolyte and a cation exchange layer (CEL).

Ion transport will happen only in the direction of the electrodes or the CEL, so the problem is understood to be one dimensional. Each region in the cell (left and right electrolyte and membrane) has length  $L$ .

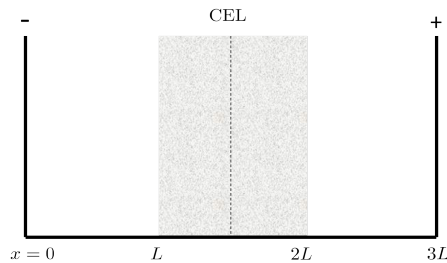


Figure 9: General layout of the cell. The cell contains three regions of length  $L$ .

Because the researched cell is relatively small, convection is neglected. Furthermore, everywhere in the cell, there must be electroneutrality. So (11)

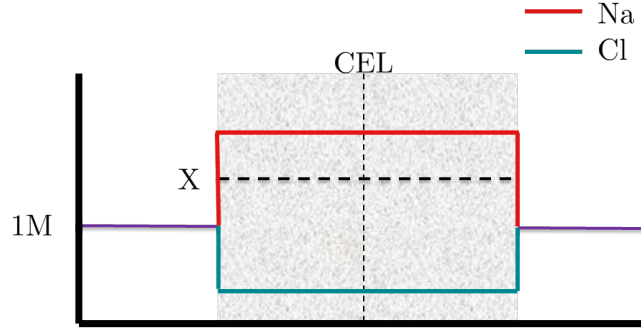


Figure 10: Initial condition of the cell, the situation where no electric field is applied. Outside of the membrane, the  $Na^+$  and  $Cl^-$  concentrations are equal, while they differ in the membrane. The exact values inside the membrane are given by (15) and (16).

should hold outside of the membrane and (12) should hold inside the membrane. This means that if one of the  $Na^+$  or  $Cl^-$  concentrations is known, then the other is known as well. Therefore, the model will only be concerned with computing the  $Na^+$  concentrations in the cell. So from now on, if concentrations are mentioned in this chapter, then these refer to  $Na^+$  concentrations. The  $Cl^-$  concentrations are then fixed and can be calculated making use of the electroneutrality conditions (11) and (12).

## 3.2 Physical Model

### 3.2.1 Initial Condition: no electric field

To understand what happens with the profile concentrations, first a cell without applied electric field is researched. Then the concentrations outside of the membrane are expected to be constant and inside of the membrane they are also constant, but different, depending on the fixed charge concentration of the membrane. The exact values are given by (15) and (16). This situation is sketched in figure 10. This forms the initial condition of the model.

### 3.2.2 Partial Differential Equation for the concentration

Now an electric field  $\Delta V$  is applied. Far enough from the electrodes, the potential is linear, while also having a jump at the solution/membrane-interfaces. This is due to the Donnan potential, described by (17). The potential profile is shown in figure 11.

To describe the concentration changes of an ion in the transient regime, the Nernst-Planck equation (7) and continuity equation (23) are combined.

$$\frac{\partial c}{\partial t} = -\frac{\partial J}{\partial x} = D \frac{\partial^2 c}{\partial x^2} + \frac{zF}{RT} D \frac{\partial c}{\partial x} \frac{\partial \phi}{\partial x} + \frac{zF}{RT} D c(x) \frac{\partial^2 \phi}{\partial x^2} \quad (36)$$

In this equation,  $c(x)$  denotes the concentration ( $\text{mol m}^{-3}$ ) at position  $x$ ,  $D$  is the diffusion coefficient of the ion,  $z$  is the charge sign (+/-),  $F$  is Faraday's constant,  $R$  the gas constant,  $T$  is the temperature (K) and  $\phi$  denotes the electric potential. Because only  $Na^+$  is considered here,  $z = +1$ . Furthermore,  $f \equiv \frac{F}{RT}$

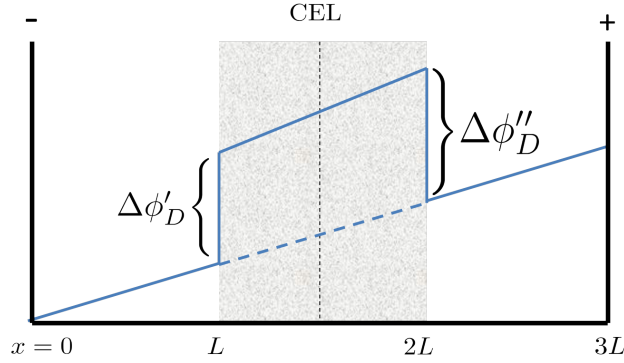


Figure 11: Because of Donnan potentials, the potential gradient inside the membrane is different from that outside of it.

is introduced for a tidier notation:

$$\frac{\partial c}{\partial t} = D \frac{\partial^2 c}{\partial x^2} + fD \frac{\partial c}{\partial x} \frac{\partial \phi}{\partial x} + fDc(x) \frac{\partial^2 \phi}{\partial x^2} \quad (37)$$

It is, however, not possible to define a derivative of a function in a point where it is discontinuous. This means that (37) is not valid at the membrane/solution-interfaces, the points  $x = L, 2L$ , because both the concentration and the potential gradients are not continuous. The solution to this problem is to divide the cell into three different regions, two electrolyte regions and the membrane:

Region I	$0 < x < L$
Region II	$L < x < 2L$
Region III	$2L < x < 3L$

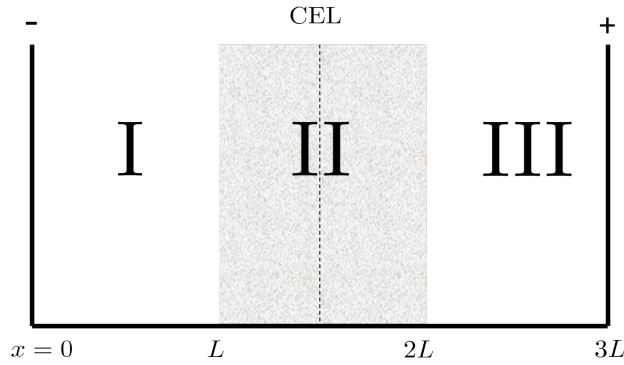


Figure 12: The cell is split into three regions of length  $L$ .

Now (37) is valid on the interior of all three regions. Furthermore, the potential is linear on each region. So the first derivative is constant:  $\frac{\partial \phi}{\partial x} \equiv E$  and the second derivative is equal to zero.  $E$  has different values in different regions. In the electrolyte regions I and II, this value is equal to  $E = \frac{\Delta V}{3L}$ . In the membrane

region II, it has a different value  $\bar{E}$ , dependent on the Donnan potentials across the interfaces:

$$\bar{E} = E + \frac{\Delta\phi_D'' - \Delta\phi_D'}{L} \quad (38)$$

Using this, (37) can be simplified:

$$\frac{\partial c}{\partial t} = D \frac{\partial^2 c}{\partial x^2} + fDE \frac{\partial c}{\partial x} \quad (39)$$

for  $0 < x < L$  and  $2L < x < 3L$ , outside the membrane. And inside the membrane:

$$\frac{\partial \bar{c}}{\partial t} = \bar{D} \frac{\partial^2 \bar{c}}{\partial x^2} + f\bar{D}\bar{E} \frac{\partial \bar{c}}{\partial x} \quad (40)$$

for  $L < x < 2L$ . Where again a bar denotes the value of a constant or concentration inside the membrane. These equations describe the concentrations inside the three regions, but not on the edges  $x = 0, L, 2L, 3L$ . The concentrations in these points are prescribed by the boundary conditions.

### 3.2.3 Boundary Conditions

The membrane is expected to have a diffusion boundary layer (DBL), a thin layer around the cell, where the concentrations are influenced by the CEL. So outside of the DBL, the concentrations remain unchanged. Then if  $L$  is chosen 'large enough', i.e. larger than the DBL, the concentrations at the edges are equal to the original concentration  $C_0$ . This forms the boundary condition at the edges of the cell:

$$c(x = 0, 3L) = C_0 \quad \text{at all times} \quad (41)$$

Now the boundary conditions at the interfaces  $x = L, 2L$  are more difficult. A valid assumption is that all ions exiting the first region on the right side, must enter the second region on the left side. This is to say that the flux at the left side of the interface must be equal to the flux on the right side of the interface. Or in more mathematical terms, the flux must be continuous:

$$J(x = L^-) = \bar{J}(x = L^+) \quad (42)$$

$$\bar{J}(x = 2L^-) = J(x = 2L^+) \quad (43)$$

Now that for each region a PDE (39) and (40), an initial condition and boundary conditions (41)-(43) are obtained, the problem is well defined and can be translated into a numerical model. However, there are some extra equations needed at the interface, because the concentration is discontinuous there. These will be analyzed in 3.3.5.

## 3.3 Numerical Model

### 3.3.1 Discretization of the system

Each region is discretized in  $n$  pieces with width  $\Delta x = \frac{3L}{3n} = \frac{L}{n}$ . Furthermore, derivatives are approximated using a central difference method:

$$\frac{\partial c}{\partial x} \approx \frac{c_{i+1} - c_{i-1}}{2\Delta x}, \quad \frac{\partial^2 c}{\partial x^2} \approx \frac{c_{i+1} - 2c_i + c_{i-1}}{\Delta x^2} \quad (44)$$

Here the subscript denotes the x-coördinate:  $c_i \equiv c(x = i\Delta x)$ . Substituting these in the PDEs (39) results, after some rearrangements, in the following:

$$\left(\frac{\partial c}{\partial t}\right)_i = \frac{D}{\Delta x^2} [(1 - fE\Delta x/2)c_{i-1} - 2c_i + (1 + fE\Delta x/2)c_{i+1}] \quad (45)$$

A similar result holds for (40). Again, the subscript denotes the x-position, so  $(\frac{\partial c}{\partial t})_i = \frac{\partial c}{\partial t}(x = i\Delta x)$ . The three regions will be considered separately.  $c1, c2, c3$  describe the concentrations in region I, II and III respectively. The last entry of  $c1$  and the first of  $c3$  are exactly on the boundaries,  $x = L$  and  $x = 2L$ . On these boundaries however, there is a discontinuity in the concentration, which means there should be two different values for the concentrations. The membrane concentrations on the boundary are therefore denoted as  $\bar{c}1_n$  and  $\bar{c}3_1$ , see figure 13.

:

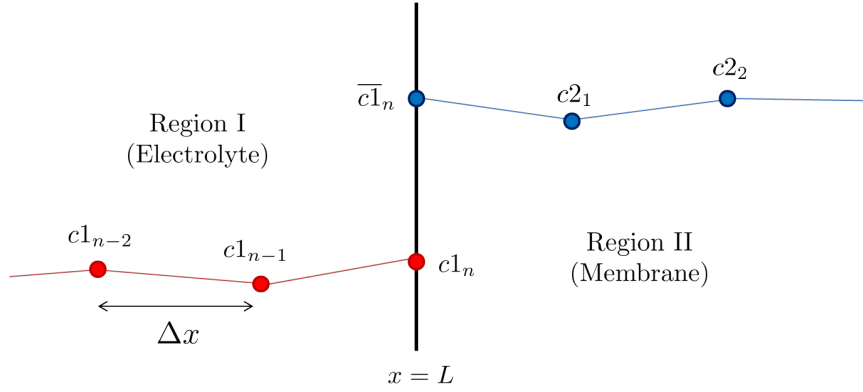


Figure 13: Discretization at the electrolyte/membrane interface.

The concentrations on the interior of the three regions are computed using the Euler forward method and (45), while the concentrations on the membrane/electrolyte interfaces are calculated using conditions (42) and (43).

### 3.3.2 Region I

First region I is examined. The concentrations in this region are denoted as an  $n \times 1$  vector  $\mathbf{c1}$ , where the entries correspond to the positions. The first  $n - 1$  points are computed using the Euler forward method in combination with (45), while the last point  $\mathbf{c1}_n$  follows from the boundary conditions. So the concentrations in the next time step are calculated as follows:

$$\mathbf{c1}(t + \Delta t)_i = \mathbf{c1}(t)_i + \Delta t \left(\frac{\partial \mathbf{c1}}{\partial t}\right)_i \quad (46)$$

where  $i = 1, \dots, n - 1$ . So it is necessary to calculate the values of  $\Delta t \frac{\partial \mathbf{c1}}{\partial t}$ , which can be done using (45).

$$\Delta t \left(\frac{\partial \mathbf{c1}}{\partial t}\right)_i = \frac{D\Delta t}{\Delta x^2} [(1 - fE\Delta x/2)c1_{i-1} - 2c1_i + (1 + fE\Delta x/2)c1_{i+1}] \quad (47)$$

$$= \alpha [(1 - \beta/2)c1_{i-1} - 2c1_i + (1 + \beta/2)c1_{i+1}] \quad (48)$$





### 3.3.5 Electrolyte/membrane interface

The concentrations at the interface are calculated differently from the concentrations in the interior of region I and III. At the interface, the concentrations are computed using the boundary conditions of continuous flux (42) and (43) in combination with (15). First, the left interface is examined, see figure 13. The concentrations  $c1_n$  and  $\bar{c1}_n$  are linked by (15):

$$\bar{c1}_n = \frac{1}{2}(\sqrt{X^2 + 4c1_n^2} + X) \quad (61)$$

Furthermore, there must be continuous flux across the interface.

$$J(x = L^-) = \bar{J}(x = L^+) \quad (62)$$

Using the Nernst-Planck equation (7), this results in the following equality:

$$-D\left[\frac{\partial c}{\partial x}(L) + fEc(L)\right] = -\bar{D}\left[\frac{\partial \bar{c}}{\partial x}(L) + f\bar{E}\bar{c}(L)\right] \quad (63)$$

Because of the discontinuity in the concentration, a central difference approximation cannot be used to approximate  $\frac{\partial c}{\partial x}$ . Instead, a backward difference is chosen for the left side, while a forward difference is used for the right side. Using the notation above, the following result is then obtained:

$$-D\left[\frac{c1_n - c1_{n-1}}{\Delta x} + fEc1_n\right] = -\bar{D}\left[\frac{c2_1 - \bar{c1}_n}{\Delta x} + f\bar{E}\bar{c1}_n\right] \quad (64)$$

The concentrations  $c1_n$  and  $c2_1$  can be computed as in subsection 3.3.2 and 3.3.4. The unknowns in the equation above are then  $c1_n$  and  $\bar{c1}_n$ . If (61) is substituted for  $\bar{c1}_n$ , it is possible to solve for  $c1_n$ .

In the same manner, it is possible to calculate the concentrations at the other interface.

Using sections 3.3.2-3.3.5, all concentrations in the electrolyte, membrane and on the interface can be computed. After each time step, the new values for the Donnan potentials are calculated with (17). Based on these potentials, the value of the electric potential gradient inside the membrane ( $\bar{E}$ ) is updated as well.

This model has not come about at once. Instead, it is the result of changing and fine tuning previous versions. One of these previous versions is added as an appendix. In appendix A, a similar model is developed as the one above, except for a different implementation of the continuous flux condition at the membrane interfaces. Furthermore, that version uses the backwards Euler method instead of the forward.

## 4 Results

In the previous section, the physical model is described, as well as how to translate this into a numerical model. This section will show the results of that model. All computations are done in Matlab and the code is included in the appendix.

### 4.1 Parameters

To do the calculations, the right values of the parameters are needed, these are shown in the following table 1.

$L$	length of each compartment	100	$\mu\text{m}$
$n$	amount of grid points per compartment	50	
$D$	diffusion coefficient of $Na^+$ outside the membrane	$10^{-8}$	$\text{m}^2/\text{s}$
$\bar{D}$	diffusion coefficient of $Na^+$ inside the membrane	$10^{-9}$	$\text{m}^2/\text{s}$
$X$	fixed charge concentration of the membrane	2	M
$C_0$	bulk concentration of the electrolyte	1	M
$\Delta t$	size of the time step	0.001	s

*Table 1: The values of the parameters used in the model described in section 3.*

These are not exact values, but are all in the right order of magnitude for the system [2],[4]. Next to these parameters, also some physical constants are used: Faraday's constant  $F$  (96485 C/mol), the ideal gas constant  $R$  (8.314 J/K mol) and the temperature  $T$  (298K, room temperature). The values of table 1 result in a step size  $\Delta x$  of  $\frac{L}{n} = 2\mu\text{m}$ . The initial membrane concentration is approximately 2.4M, according to (15).

## 4.2 No Applied Potential

First, a situation with no applied potential is considered. For the potential gradient, this means that  $E = \bar{E} = 0$ . The results are shown in figure 14 From

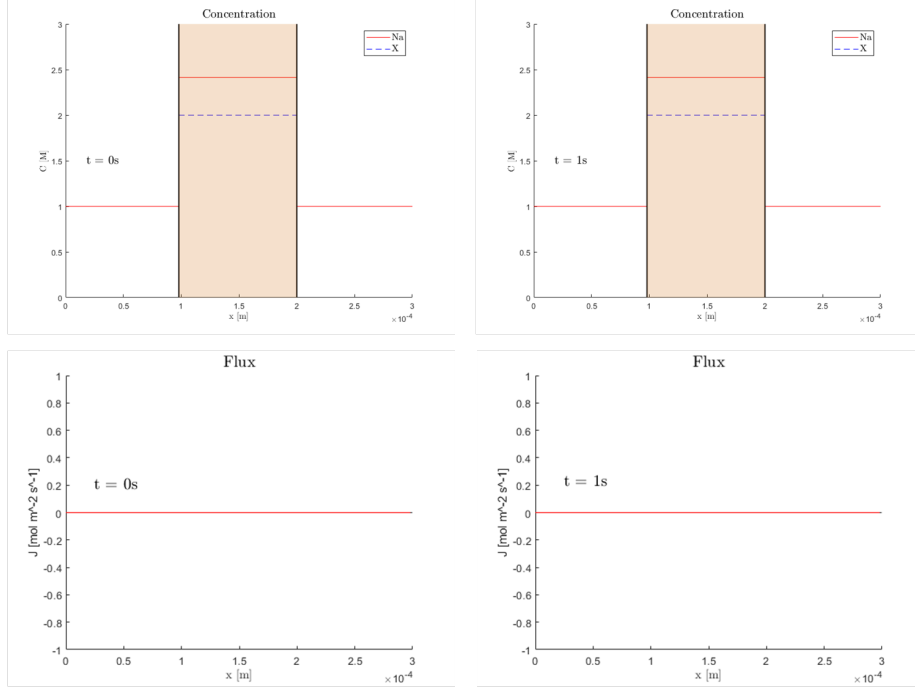


Figure 14: The concentrations and flux at  $t = 0s$  and  $t = 1s$ , when there is no applied potential.

this figure 14 it is clear that the results do not vary from the initial condition, as the flux is zero everywhere at all times.

## 4.3 Applied Potential

Now a situation where there is an applied potential is simulated. The value for this potential is  $\Delta V = 1V$ . For the electric potential gradient  $E = \frac{\partial \phi}{\partial x}$  this means that it equals  $\frac{\Delta V}{3L} \approx 3.33V/m$ . The fact that  $E$  is positive, indicates that the positive electrode is on the right side and the negative electrode on the left.

Because there is a potential applied, ions are not only transported by diffusion, but also migration. The model aims to show how the concentration will change over time as a result of this diffusion and migration.

Firstly, the  $Na^+$  concentrations at times  $t = 0.000, 0.002, \dots, 0.010s$  are shown in figure 15. The first thing that stands out in these results is that  $Na^+$  ions accumulate at the right interface, on the side of the positive electrode. At the same time, the concentrations at the left interface are depleted. To get a better understanding as to why this happens, the flux is researched. Figure 16 shows the flux at time  $t = 0.006s$  Before continuing, there are some remarks on this plot. The figure shows not only the total flux (dashed line), but also the individual

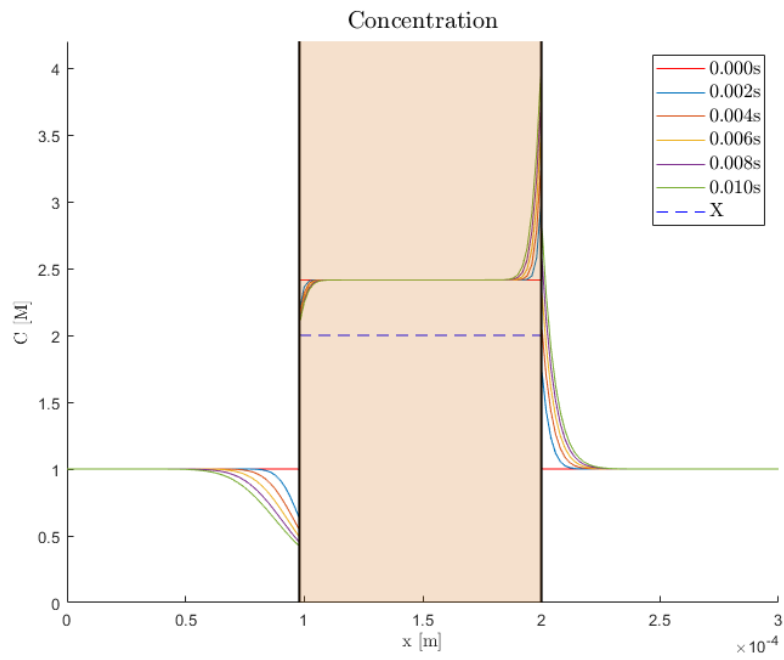


Figure 15: The  $\text{Na}^+$  concentrations at  $t = 0.000, 0.002, \dots, 0.010$ s.

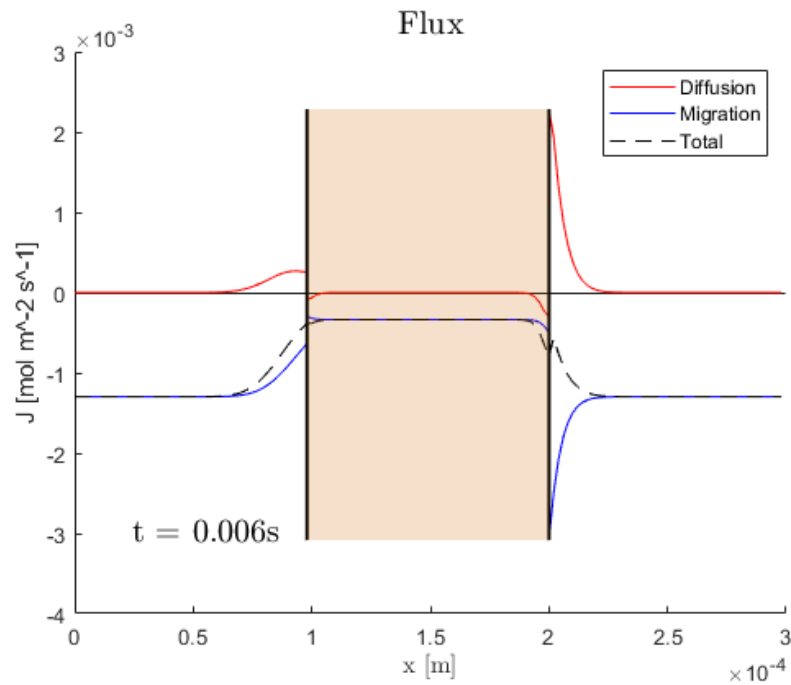


Figure 16: The flux at  $t = 0.006$ s. Next to the total flux, the figure also shows the separate contributions to the flux from both diffusion and migration.

contributions of both diffusion (red) and migration (blue). These are physically given by

$$\begin{aligned} J_{diffusion} &= -D \frac{\partial c}{\partial x} \\ J_{migration} &= -DfEc(x) \\ J_{total} &= J_{diffusion} + J_{migration} \end{aligned}$$

Note that inside the membrane,  $\bar{D}$  and  $\bar{E}$  are used instead of  $D$  and  $E$  respectively. In the points not on the membrane/solution interface or the edge,  $\frac{\partial c}{\partial x}$  is calculated using a central difference approximation. On the interfaces and edges, however, this is not possible. In these points, either a forward or backward difference is used, depending on which side of the interface or edge a point is. Because of these different approximations, there seems to be a discontinuity in the diffusion flux (and thus the total flux also) at the points next to the interfaces. These discontinuities are especially visible at the right side of the right membrane, but only arise from a numerical inaccuracy, i.e. a different approximation technique. Furthermore, it is clear from the plot that the continuous flux condition is satisfied: there is no jump in the dashed line at the membrane interfaces.

While there is lots of activity around the interfaces, away from these interfaces, the concentrations remain largely unchanged. The concentration changes have not yet 'reached' these areas. It would be interesting to see what happens at later times. Figure 17 shows the concentrations at intervals of 0.02 seconds, up to a time of  $t = 0.1s$ .

The accumulation at the right side and depletion on the left side seems to go on, with a concentration reaching almost 12M at  $t = 0.1s$ . Also, in figure 17 there are more positions where the concentration changes. There is activity in half of the membrane and also in the left electrolyte. The right half of the right electrolyte still remains unchanged, but the unchanged area is smaller than in figure 15.

The flux at  $t = 0.06s$  is shown in figure 18. Figure 18 is similar to figure 16 ( $t = 0.006s$ ). The main difference is that the values of the flux are higher in figure 18, where the maximum value of the migrational flux is more than  $-0.07 \text{ mol m}^{-2} \text{ s}^{-1}$ . This is about 20 times higher than at  $t = 0.006s$ , where the migrational flux reached a value of around  $-3 \cdot 10^{-3} \text{ mol m}^{-2} \text{ s}^{-1}$ .

These results will be discussed in the next section.

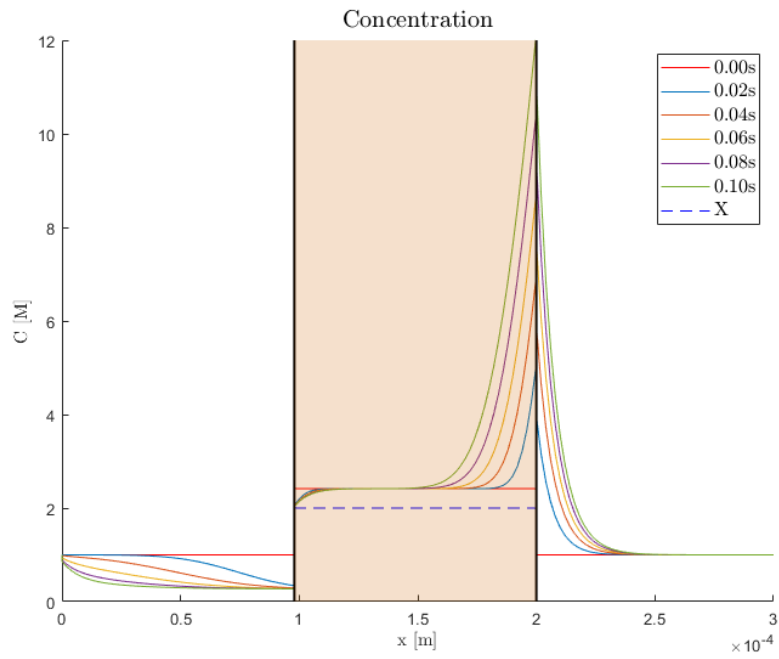


Figure 17:  $\text{Na}^+$  concentrations at times  $t = 0, 0.02, \dots, 0.10\text{s}$ .

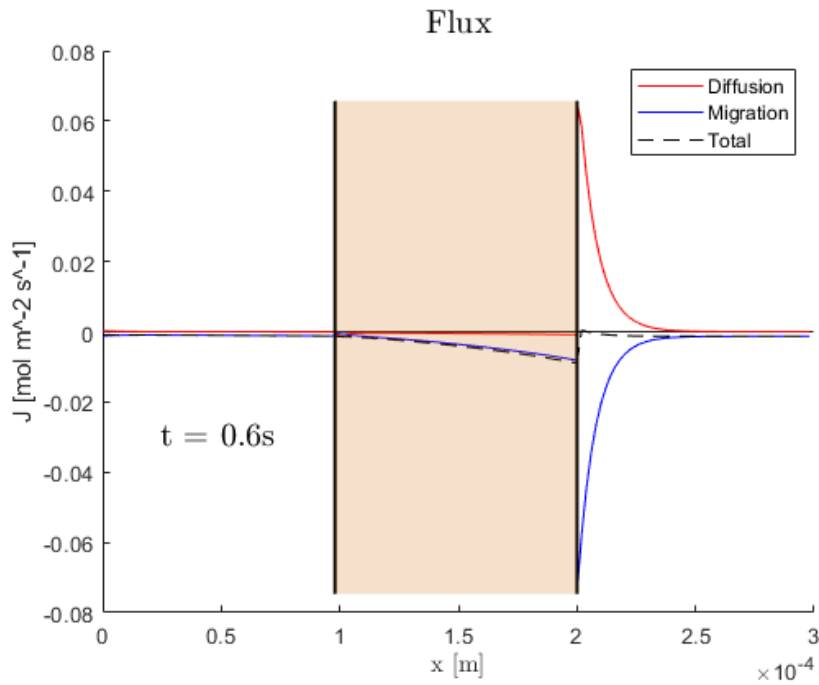


Figure 18: The diffusional, migrational and total flux at  $t = 0.06\text{s}$ .

## 5 Discussion

### 5.1 No applied potential

Figure 14 shows both the concentrations and flux at  $t = 0s$  and  $t = 1s$  in the absence of an applied potential. There has been no change in concentration in this period and the flux equals zero everywhere. This is exactly the expected result. Because there is no applied potential, there is no migration. The only ion transport is then due to diffusion. In all three regions, however, the concentrations are equal. There is no concentration gradient and hence no diffusion. All concentrations will stay the same.

### 5.2 Applied Potential

First the results of figure 16 will be discussed. Relevant in this discussion is the continuity equation (23), which links the flux to the concentration changes:

$$\frac{\partial c}{\partial t} = -\frac{\partial J}{\partial x}$$

Simply put, this means that a negative slope of the total flux equals a rise in concentration, while a positive slope equals a drop. This is in agreement with figure 15: left of the membrane the (total) flux has a positive slope and the concentration there falls, while at the right side of the membrane the opposite applies.

Also remember that the flux is due to diffusion and due to migration:

$$\begin{aligned} J_{diffusion} &= -D \frac{\partial c}{\partial x} \\ J_{migration} &= -D f E c(x) \\ J_{total} &= J_{diffusion} + J_{migration} \end{aligned}$$

Furthermore, a positive flux indicates ion movement to the right, while a negative flux implies ion transport to the left. Remarkable about figure 16 is the quite big discrepancy between the flux due to diffusion and that due to migration at the right side of the membrane. This area will be researched in more detail. On one hand, diffusion causes the ions to travel to the right (the diffusional flux is positive), which makes sense considering there are more ions to the left than to the right. On the other hand, migration drives the ions to the left (negative flux). This is in agreement with the fact that  $Na^+$  ions are positive and the positive electrode is to the right and negative electrode to the left. The migrational flux is bigger however, which causes the ions to move to the left. Also, the slope of the total flux is negative which signifies an accumulation of ions. On top of this, the slope becomes greater (i.e. more negative), closer to the membrane. This means that the concentrations rises faster closer to the membrane. This has in turn two consequences for the migrational flux and the diffusional flux.

Because the migrational flux is proportional to concentration, this migrational flux will rise if the concentration rises. And because the concentrations rise faster closer to the membrane, the migrational fluxes also become bigger closer to the membrane. This means that the difference in migrational fluxes, i.e. the

slope, becomes bigger. This causes the concentrations in turn to rise even harder. As a result, the migrational flux becomes even bigger, the slope increases more, concentrations get even bigger, etc.

For diffusion, a similar process happens. Concentrations rise faster near the membrane, which causes the difference in concentrations to be bigger also. This means that  $\frac{\partial c}{\partial x}$ , or the concentration slope, becomes bigger and thus the diffusional flux as well. Although, this diffusional flux is opposite to the migrational flux, it is also smaller (absolutely).

So diffusion 'slows down' the concentration rise near the right side of the membrane, but ultimately, because the migrational flux is greater, an unstable equilibrium is reached. This can be seen in figure 15 and becomes even clearer when greater times are plotted, see figure 17.

At the other side of the membrane, the same mechanism is in place, although on a smaller scale. This is due to the different diffusion coefficients. Specifically, the diffusion coefficient inside the membrane is 10 times lower than outside of it, see table 1.

Figure 17 clearly shows the unstable equilibrium described above: the concentrations at the right side of the membrane continue to rise with every time step. Furthermore, the more time passes, the bigger the area where concentrations change. Especially in the left electrolyte there is a lot of change. It follows from the figures that the assumption for the left edge does not longer hold. This assumption was that, because most activity will take place in the membrane and the interfaces, the concentrations 'far away' from the membrane should remain unchanged. That means that the concentration on the left edge of the cell should stay equal to the bulk concentration  $C_0 = 1M$ . From figure 17, it is clear that this is no longer valid. The concentration at the left side is now 'artificially' (numerically) held at 1M, but it should be lower, following the trend of the other concentrations in the left electrolyte. At this moment the model breaks down, as it is no longer consistent with the assumptions. Simulating any later time step will then not result in meaningful information.

Furthermore, it is clear that the results of this model are not physical. In one point for example, after only 0.1s, the concentration reaches a value of 12M. This is certainly not physically possible. That means there are some inaccuracies or errors in the model. The discussion above however, shows that the model is in agreement with what one would expect to happen physically. It is understood how a certain concentration profile, causes a certain flux, and how a certain flux changes the concentration profile, based on physical equations. The results verify these reasonings. How the concentration profile changes when going from one time step to the other, seems to be correct. Therefore it might be a good idea to reevaluate the assumptions and simplifications that were made when developing the model.

The main limitation of this model appears to be an assumption made about the potential gradient. It is assumed that the potential is linear everywhere, with a

certain slope outside the membrane and a different one inside of it. The value of the slope ( $\frac{\partial\phi}{\partial x}$ ) inside the membrane is dependent on the Donnan potentials, see (17) and figure 3. It could be, however, that this assumption is not entirely valid or too limited. The potential gradient is considered to remain constant through the bulk electrolyte, ignoring the existence of a diffusion boundary layer where different concentrations exist. Since different concentrations indicate a different mobility, also a change in the resistance should be taken into account and therefore also a change in the potential. Minimally five regions should then be distinguished in order to cope with the varying potential gradient. Two interfaces between these regions will be discontinuous as a Donnan potential should be incorporated, making the situation more complex.

## 6 Conclusion

In the situation where there is no applied potential, the model gives exactly the expected result. The flux is zero everywhere in the cell and the concentrations do not differ from the initial condition.

When there is a potential applied, however, the model gives a different result.  $Na^+$  ions accumulate at the side of the membrane that is closest to the positive electrode, while they dissipate at the other side of the membrane. This process of accumulation and depletion can be deduced and predicted from plots of both concentration and flux, in combination with the physical expressions. This leads to the belief that the model is consistent with the physics that describe the model and the assumptions that have been made. However, this accumulation is amplified at every time step, which results in a  $Na^+$  concentration of almost 12M after only 0.10 seconds, while it started with a concentration of 1M. This is of course not possible in real life and a result one would not expect. Hence, there appears to be an assumption that is not entirely valid or too limited.

It is thought that that assumption is the one about the electric potential. In the model, this electric potential is assumed to be linear, with two different values for the gradient: one value outside of the membrane and a different value inside the membrane. This ignores however the diffusion boundary layers, the layers just on the outsides of the membrane. It is believed that the potential gradient in these areas has another, different value. That means the model should account for five different regions (one membrane, two diffusion boundary layers, two bulk solutions in the electrolytes at the outside) as opposed of the three regions it uses now. At the electrolyte/membrane interfaces, there is also a Donnan potential, however, which causes a discontinuity in both concentrations and potential there. Integrating these five regions would then result in a much more complex model, but one that would be more accurate, especially around the electrolyte/membrane interfaces.

## References

- [1] Toshikatsu Sata. *Ion Exchange Membranes*. The Royal Society of Chemistry, 2004.
- [2] Allen J. Bard and Larry R. Faulkner. *Electrochemical Methods: Fundamentals and Applications*. John Wiley & Sons, Inc, 2001.
- [3] Harrie van den Akker and Rob Mudde. *Fysische transportverschijnselen: denken in balansen*. Delft Academic Press, 2014.
- [4] L.P.B.M. Janssen and M.M.C.G. Warmoeskerken. *Transport Phenomena Data Companion*. VSSD, 2006.
- [5] K.N. Mani. Electrodialysis water splitting technology. *Journal of Membrane Science*, 58(2):117 – 138, 1991.
- [6] Astom corporation. <http://www.astom-corp.jp/en/product/02.html>. Accessed: 2019-02-07.
- [7] Cradle. <https://www.cradle-cfd.com/tec/column01/012.html>. Accessed: 2019-06-04.
- [8] M.B. van Gijzen M.J. Vuik C. Vuik, F.J. Vermolen. *Numerical Methods for Ordinary Differential Equations*. Delft Academic Press, 2016.
- [9] E. Süli and D. Mayers. *An Introduction to Numerical Analysis*. Cambridge university Press, 2003.
- [10] Philippe Sistat and Gérald Pourcelly. Chronopotentiometric response of an ion-exchange membrane in the underlimiting current-range. Transport phenomena within the diffusion layers. *Journal of Membrane Science*, 123(1):121–131, 1997.
- [11] Michele Tedesco, Andrea Cipollina, Alessandro Tamburini, I. David L. Bogle, and Giorgio Micale. A simulation tool for analysis and design of reverse electrodialysis using concentrated brines. *Chemical Engineering Research and Design*, 93(May):441–456, 2015.
- [12] M. Tedesco, H. V.M. Hamelers, and P. M. Biesheuvel. Nernst-Planck transport theory for (reverse) electrodialysis: I. Effect of co-ion transport through the membranes. *Journal of Membrane Science*, 510:370–381, 2016.

## Appendix A

In this section a different approach to the model is presented. The model development is mostly the same, but the numerical methods are different. The most important changes are a different implementation of the continuous flux condition at the membrane interfaces and the model uses the backward Euler method instead of the forward. This backward Euler method results in an implicit, nonlinear expression for the concentrations, which are solved using a Newton-Raphson approximation.

For continuous flux at the left membrane, the following holds:

$$J(x = L^-) = \bar{J}(x = L^+)$$

or, using the Nernst-Planck equation:

$$-D\left[\frac{\partial c}{\partial x}(L) + fEc(L)\right] = -\bar{D}\left[\frac{\partial \bar{c}}{\partial x}(L) + f\bar{E}\bar{c}(L)\right] \quad (65)$$

Next to this expression, the concentration just inside the membrane is linked to the concentration just outside of it by (15):

$$\bar{c}(L) = \frac{1}{2}\left(\sqrt{X^2 + 4c(L)^2} + X\right) \quad (66)$$

Combining these two yields the following expression:

$$\frac{\partial c}{\partial x}(L) = f\frac{DEc(L) - \bar{D}\bar{E}\bar{c}(L)}{\bar{D}\frac{2c(L)}{\sqrt{X^2 + 4c(L)^2}} - D} \quad (67)$$

Now, the partial derivative on the left hand side of this equation is replaced by its discretized counterpart ( $c(L)$  corresponds to  $c1_n$ ), such that an expression for the virtual point  $c1_{n+1}$  is obtained:

$$c_{n+1} = 2\Delta x f \frac{DEc_n - \bar{D}\bar{E}\bar{c}_n}{\bar{D}\frac{2c_n}{\sqrt{X^2 + 4c_n^2}} - D} + c1_{n-1} \quad (68)$$

where  $\bar{c}_n$  is defined as follows:

$$\bar{c}_n = \frac{1}{2}\left(\sqrt{X^2 + 4c_n^2} + X\right) \quad (69)$$

This  $c_{n+1}$  can be used to determine  $(\frac{\partial c1}{\partial t})_n$  and subsequently  $c1_n$  in the next time step.

Now because the backward Euler method is used, an implicit expression for  $\frac{\partial c}{\partial t}$  is obtained:

$$\begin{aligned} c^{j+1} &= c^j + \Delta t \left(\frac{\partial c}{\partial t}\right)^{j+1} \\ c^{j+1} - c^j - \Delta t \left(\frac{\partial c}{\partial t}\right)^{j+1} &= 0 \end{aligned}$$

Where the superscript  $j$  indicates the time step:  $c^j = c(t = j\Delta t)$  Here the only unknown is the vector  $c^{j+1}$  (because  $g^{j+1}$  is dependent on  $c_n^{j+1}$ ). The root problem above can be solved with a Newton-Raphson approximation. The starting point is the concentration of the previous time step  $c^j$  and the stopping criterion is when the difference between two subsequent approximations is very small.

The error in this approach is the step from (65) to (67). There the (analytical) derivative of (66) is computed, while (66) is not really a function of  $x$ . The approach taken in the section 3, using one sided numerical derivatives, seems therefore better. Originally, it was the intention to use the backward Euler method, in combination with Newton-Raphson approximation there as well, in order to guarantee stability. But for some reason the Newton-Raphson approximation did not converge. Now the (explicit) forward Euler method is used, which works fine, as long as  $\Delta t$  is kept small.

## Appendix B: Matlab Code

```
1 clc,clear all
2 %% Whole region
3 %BC:      Bulk concentration = 1
4 %         Continuous Flux at interface
5 %         Forward difference: explicit
6 %% Constants
7 D = 1e-8;   %m^2/s
8 DM = 1e-9;  % inside membrane
9 z_Na = 1;
10 z_Cl = -1;
11 % f
12 F = 96485.3329;    %C/mol
13 R = 8.314;         %J/(mol K)
14 T = 298;          %K
15 f = F/(R*T);      %C/J=V^-1
16 %% Parameters
17 C0 = 1; %start concentration of electrolyte
18 X = 2; %fixed concentration of membrane
19 L = 10^-4; %length of each compartment = 100um
20 n = 50; %discretization of x
21 dx = L/(n);
22 x1 = dx*(0:(n-1));
23 x2 = L + x1;
24 x3 = 2*L + x1;
25 x = [x1 x2 x3];
26 V_0= 1; %applied voltage
27 E = V_0/(3*L); %potential gradient (d\phi / dx)
28
29 %% Initial conditions
30 CM = (sqrt(X^2+4*C0^2)+X)/2;
31 c1(:, :, 1) = C0*ones(n,1); %concentrations on the
    left side
32 c2(:, :, 1) = CM*ones(n,1); %concentrations in the
    middle (membrane)
33 c3(:, :, 1) = C0*ones(n,1); %concnetrations right side
34 c(:, :, 1) = [c1; c2; c3];
35 cnm(1) = CM;
36 cmm(1) = CM;
37
38
39 %% Build matrices
40 m = 10001;
41 dt = 0.0001; %must be small!
42
43 %some constants
44 alfa = D*dt/dx^2;
45 beta = f*E*dx;
```

```

46 EM(1) = E;
47
48 %discretization matrix for left electrolyte
49 A = zeros(n-1,n);
50 A1 = -2*alfa*eye(n-1,n);
51 A2 = alfa*(1+beta/2)*[zeros(n-1,1),eye(n-1)]; %right
diag
52 A3 = alfa*(1-beta/2)*[zeros(1,n);eye(n-2,n)]; %left
diag
53 A = A + A1 + A2 + A3;
54
55 %discretization matrix for right electrolyte
56 CC = zeros(n-1,n);
57 CC1 = -2*alfa*[zeros(n-1,1), eye(n-1)]; %diag
58 CC2 = alfa*(1+beta/2)*[zeros(n-1,2),eye(n-1,n-2)]; %
right diag
59 CC3 = alfa*(1-beta/2)*eye(n-1,n); %left diag
60 CC = CC + CC1 + CC2 + CC3;
61
62 %% Time integration
63 for j = 2:m
64     %new constants, inside membrane
65     Em = EM(j-1);
66     alfa_m = DM*dt/dx^2;
67     beta_m = f*Em*dx;
68
69     %discretization matrix for membrane
70     B = zeros(n,n);
71     B1 = -2*alfa_m*eye(n,n);
72     B2 = alfa_m*(1+beta_m/2)*[zeros(n,1), eye(n,n-1)]; %
right diag
73     B3 = alfa_m*(1-beta_m/2)*[zeros(1,n); eye(n-1,n)]; %
left diag
74     B = B + B1 + B2 + B3;
75
76     %calculate concentrations in new timestep
77     c1(1:n-1,:,j) = c1(1:n-1,:,j-1) + A*c1(:,j-1) +
[alfa*(1-beta/2)*C0;zeros(n-2,1)]; %left
78
79     c2(1:n,:,j) = c2(:,j-1) + B*c2(:,j-1);
80     c2(1,1,j) = c2(1,1,j) + alfa_m*(1-beta_m/2)*c_nm(j-1)
; %middle
81     c2(n,1,j) = c2(n,1,j) + alfa_m*(1+beta_m/2)*c_mm(j-1)
;
82
83     c3(2:n,:,j) = c3(2:n,:,j-1) + CC*c3(:,j-1) + [
zeros(n-2,1);alfa*(1+beta/2)*C0]; %right
84
85     %solve for the concentrations along membrane

```

```

86     %satisfies a) Donnan condition and b) continuous
      flux across interface
87     % k and m are some constants, derivation in
      notebook
88
89     k1 = -2*(D/dx+D*f*E)/(DM/dx-f*Em*DM);
90     k2 = 2*( DM/dx*c2(1,1,j) + D/dx*c1(n-1,1,j) )/(DM/
      dx-f*Em*DM) - X;
91
92     c1(n,1,j) = -sqrt( k1^2*k2^2 - (k1^2-4)*(k2^2-X^2)
      ) - k1*k2;
93     c1(n,1,j) = c1(n,1,j)/ (k1^2 - 4); %concentration
      in electrolyte
94     cnm(j) = 0.5*(sqrt(X^2+4*c1(n,1,j)^2)+X); %
      concentration in membrane
95
96     m1 = -2*(D/dx-f*D*E)/(DM/dx+f*DM*Em);
97     m2 = 2*(DM/dx*c2(n,1,j)+D/dx*c3(2,1,j));
98     m2 = m2/ (DM/dx + f*DM*Em)-X;
99
100    c3(1,1,j) = -sqrt( m1^2*m2^2 - (m1^2-4)*(m2^2-X^2)
      ) - m1*m2;
101    c3(1,1,j) = c3(1,1,j)/ (m1^2-4); %concentration in
      electrolyte
102    cmm(j) = 0.5*(sqrt(X^2+4*c3(1,1,j)^2)+X); %
      concentration in membrane
103
104    %calculate the Donnan potentials and the new value
      for the potential
105    %gradient inside the membrane
106    dp1(j) = R*T/F*log(cnm(j)/c1(n,1,j)); %left side
107    dp2(j) = R*T/F*log(c3(1,1,j)/cmm(j)); %right side
108    EM(j) = E + (dp2(j)+dp1(j))/((n+2)*dx);
109
110    end
111    c = cat(1,c1,c2,c3);
112    %% Calculate total flux
113    k = 1;
114    flux0 = zeros(n);
115    flux1 = -f*E*eye(n);
116    flux1M = -f*EM(k)*eye(n);
117    flux2 = -1/(2*dx)*[zeros(n,1), eye(n,n-1)];
118    flux3 = 1/(2*dx)*[zeros(1,n);eye(n-1,n)];
119    flux = D*(flux0 + flux1 + flux2 + flux3);
120    flux(1,1) = D/dx - D*f*E;
121    flux(1,2) = -D/dx;
122    flux(n,n-1) = D/dx;
123    flux(n,n) = -D/dx - D*f*E;
124
125    fluxM0 = zeros(n+2);

```

```

126 fluxM1 = -f*EM(k)*eye(n+2);
127 fluxM2 = -1/(2*dx)*[zeros(n+2,1), eye(n+2,n+1)];
128 fluxM3 = 1/(2*dx)*[zeros(1,n+2);eye(n+1,n+2)];
129
130 fluxM = DM*(fluxM0 + fluxM1 + fluxM2 + fluxM3);
131 fluxM(1,1) = DM/dx - DM*f*EM(k);
132 fluxM(1,2) = -DM/dx;
133 fluxM(n+2,n+1) = DM/dx;
134 fluxM(n+2,n+2) = -DM/dx - DM*f*EM(k);
135
136 J1 = flux*c1(:, :, k);
137 J2 = fluxM*[cnm(k);c2(:, :, k);cmm(k)];
138 J3 = flux*c3(:, :, k);
139 %J = [flux*c1(:, :, k);fluxM*c2(:, :, k);flux*c3(:, :, k)];
140 figure()
141 hold on
142 title('Total Flux')
143 plot(x1, J1, 'r')
144 plot([x1(n), x2, x3(1)], J2, 'r')
145 plot(x3, J3, 'r')
146 %% Calculate flux separately
147 k = 6001;
148 Eflux = -f*E*D*eye(n);
149 EMflux = -f*EM(k)*DM*eye(n+2);
150
151 Dflux0 = zeros(n);
152 Dflux2 = -1/(2*dx)*[zeros(n,1), eye(n,n-1)];
153 Dflux3 = 1/(2*dx)*[zeros(1,n);eye(n-1,n)];
154 Dflux = D*(Dflux0 + Dflux2 + Dflux3);
155 Dflux(1,1) = D/dx;
156 Dflux(1,2) = -D/dx;
157 Dflux(n,n-1) = D/dx;
158 Dflux(n,n) = -D/dx;
159
160 DMflux0 = zeros(n+2);
161 DMflux2 = -1/(2*dx)*[zeros(n+2,1), eye(n+2,n+1)];
162 DMflux3 = 1/(2*dx)*[zeros(1,n+2);eye(n+1,n+2)];
163
164 DMflux = DM*(DMflux0 + DMflux2 + DMflux3);
165 DMflux(1,1) = DM/dx;
166 DMflux(1,2) = -DM/dx;
167 DMflux(n+2,n+1) = DM/dx;
168 DMflux(n+2,n+2) = -DM/dx;
169
170 JD1 = Dflux*c1(:, :, k);
171 JD2 = DMflux*[cnm(k);c2(:, :, k);cmm(k)];
172 JD3 = Dflux*c3(:, :, k);
173
174 JE1 = Eflux*c1(:, :, k);
175 JE2 = EMflux*[cnm(k);c2(:, :, k);cmm(k)];

```

```

176 JE3 = Eflux*c3(:, :, k);
177
178 J1 = JD1 + JE1;
179 J2 = JD2 + JE2;
180 J3 = JD3 + JE3;
181
182 J = [J1; J2; J3];
183 JD = [JD1; JD2; JD3];
184 JE = [JE1; JE2; JE3];
185 y1 = min([min(J), min(JD), min(JE)]);
186 y2 = max([max(J), max(JD), max(JE)]);
187
188 figure()
189 hold on
190 title('Flux', 'Interpreter', 'LaTeX', 'fontsize', 15)
191 plot(x1, JD1, 'r')
192 plot(x1, JE1, 'b')
193 plot(x1, J1, '--k')
194 plot([x1(n), x2, x3(1)], JD2, 'r')
195 plot(x3, JD3, 'r')
196 plot([x1(n), x2, x3(1)], JE2, 'b')
197 plot(x3, JE3, 'b')
198 plot([x1(n), x2, x3(1)], J2, '--k')
199 plot(x3, J3, '--k')
200
201 legend('Diffusion', 'Migration', 'Total')
202
203 ylabel('J [mol m-2 s-1]', 'Interpreter', 'LaTeX')%, '
    rotation', 0)
204 xlabel('x [m]', 'Interpreter', 'Latex')
205 plot([x(n), x(n)], [y1, y2], 'k', 'linewidth', 1.5, '
    HandleVisibility', 'off') %plot left side of
    membrane
206 plot([x3(1), x3(1)], [y1, y2], 'k', 'linewidth', 1.5, '
    HandleVisibility', 'off') %plot right side
207 area([x(n), x3(1)], [y2, y2], 'FaceAlpha', 0.2, 'FaceColor'
    , [0.8 0.4 0], 'EdgeColor', 'none', 'HandleVisibility',
    'off')
208 area([x(n), x3(1)], [y1, y1], 'FaceAlpha', 0.2, 'FaceColor'
    , [0.8 0.4 0], 'EdgeColor', 'none', 'HandleVisibility',
    'off')
209 T = (k-1)*dt;
210 text(x(round(n/4)), -0.03, ['t = ', num2str(T), 's'], '
    fontsize', 15, 'Interpreter', 'latex') %add simulated
    time to graph
211 %% Plot single timestep
212 k=1;
213 figure()
214 hold on
215 y = 1.2*abs(max(c(:, :, k)));

```

```

216 axis([x(1) x(3*n)+dx 0 y])
217
218 plot(x1,c1(:,:k),'r')
219 plot([x1(n),x2,x3(1)],[cnm(k);c2(:,:k);cmm(k)],'r','
    HandleVisibility','off')
220 plot([x3,x3(n)+dx],[c3(:,:k);C0],'r','
    HandleVisibility','off')
221
222 %make the figure look nicer
223 plot([x(n),x3(1)],[X,X],'b--') %plot X line
224 plot([x(n),x(n)],[0,y],'k','linewidth',1.5,'
    HandleVisibility','off') %plot left side of
    membrane
225 plot([x3(1),x3(1)],[0,y],'k','linewidth',1.5,'
    HandleVisibility','off') %plot right side
226 area([x(n),x3(1)],[y,y],'FaceAlpha',0.2,'FaceColor'
    ,[0.8 0.4 0],'EdgeColor','none','HandleVisibility',
    'off')
227 title('Concentration','Interpreter','LaTeX','fontSize'
    ,15)
228 leg1 = legend('Na','X');
229 set(leg1,'Interpreter','latex'); %edit legend
230 set(leg1,'fontSize',12);
231 ylabel('C [M]','Interpreter','Latex','%','rotation',0)
232 xlabel('x [m]','Interpreter','Latex')
233 T = (k-1)*dt;
234 text(x(round(n/5)),y/2,['t = ',num2str(T),'s'],'
    fontSize',15,'Interpreter','latex') %add simulated
    time to graph
235
236 %% Plot multiple timesteps
237
238 figure('units','centimeters','position',[5 2 20 15] )
239 hold on
240 y = 3;%1.2*abs(max(c(:,:k)));
241 axis([x(1) x(3*n)+dx 0 y])
242
243 k=1;
244
245 plot(x1,c1(:,:k),'r')
246 plot([x1(n),x2,x3(1)],[cnm(k);c2(:,:k);cmm(k)],'r','
    HandleVisibility','off')
247 plot([x3,x3(n)+dx],[c3(:,:k);C0],'r','
    HandleVisibility','off')
248
249 %make the figure look nicer
250 plot([x(n),x3(1)],[X,X],'b--') %plot X line
251 plot([x(n),x(n)],[0,y],'k','linewidth',1.5,'
    HandleVisibility','off') %plot left side of
    membrane

```

```

252 plot([x3(1),x3(1)],[0,y],'k','linewidth',1.5,'
      HandleVisibility','off') %plot right side
253 area([x(n),x3(1)],[y,y],'FaceAlpha',0.2,'FaceColor'
      ,[0.8 0.4 0],'EdgeColor','none','HandleVisibility',
      'off')
254 title('Concentration','Interpreter','LaTeX','fontsize'
      ,15)
255 %leg1 = legend('0.00s','0.02s','0.04s','0.06s','0.08s
      ','0.10s','X');
256 leg1 = legend('Na','X');
257 set(leg1,'Interpreter','latex'); %edit legend
258 set(leg1,'fontsize',12);
259 ylabel('C [M]','Interpreter','Latex')%,'rotation',0)
260 xlabel('x [m]','Interpreter','Latex')
261 T = (k-1)*dt;
262 text(x(round(n/5)),y/2,['t = ',num2str(T),'s'],'
      fontsize',15,'Interpreter','latex') %add simulated
      time to graph

```